PERFORMANCE BOUNDS FOR COOPERATIVE RSS EMITTER TRACKING USING DIFFUSION PARTICLE FILTERS

Stiven S. Dias

Embraer S.A.
São José dos Campos SP 12227-901, Brazil
+55 12 3927-5428; stiven.dias@embraer.com.br

Marcelo G. S. Bruno

Instituto Tecnológico de Aeronáutica
São José dos Campos SP 12228-900, Brazil
+55 12 3947-6906; bruno@ita.br

ABSTRACT

This paper introduces a methodology for numerical computation of the Posterior Cramér-Rao Lower Bound (PCRLB) for the position estimate mean-square error when a moving emitter is tracked by a network of received-signal-strength (RSS) sensors using a distributed, random exchange diffusion filter. The square root of the PCRLB is compared to the empirical root-mean-square error curve for a particle filter implementation of the diffusion filter, referred to as RndEx-PF, and to the square root of the PCRLB for the optimal centralized filter that assimilates all network measurements at each time instant. In addition, we also compare the proposed RndEx-PF algorithm to three alternative distributed trackers based on Kullback-Leibler fusion using both iterative consensus and non-iterative diffusion strategies.

Index Terms— Posterior Cramér-Rao Lower Bound, Particle Filters, Diffusion, RSS Sensors, Emitter Tracking.

I. INTRODUCTION

Distributed particle filtering (PF) [1] has become a standard technique for cooperative target tracking in sensor networks where each network node has computational and communication capabilities of its own. A common network cooperation strategy found in other contexts in the literature is the Kullback-Leibler (KL) fusion methodology, see e.g. [2], [3], where, at any given instant n, each node first runs a local particle filter that assimilates only the node's own current measurements. Subsequently, the network nodes run an iterative average consensus protocol [4] which, after multiple iterations, seeks to replace the local state posterior probability density functions (p.d.f's) at each node with a normalized version of the geometric mean of all node posteriors. A non-iterative, online version of the KL fusion approach was also independently introduced by Dedecius et al. in [5].

Alternatively, we introduced in [6] and [7] the non-iterative Random Exchange Diffusion Particle Filter (RndEx-PF), which, building on previous work on distributed Kalman filtering by Kar et al. [8], uses a methodology where network nodes first exchange their local posterior p.d.f's with randomly selected neighbors and then use a particle filter to assimilate all available measurements in their closed neighborhood. As shown in [7], the aforementioned algorithm builds over time, at each node, different state posterior p.d.f's conditioned on different random subsets of all network measurements, with the measurements in each of those random subsets coming from the entire network and not only from the node's immediate vicinity, thus enabling information diffusion.

In this paper, building on previous results in [9], we introduce a methodology for numerical computation of the posterior Cramér-Rao lower bound (PCRLB) for the average network mean-square state estimation error when the proposed random exchange diffusion protocol is used. The computed bound is compared, in a specific application of emitter tracking with received-signal-strength (RSS) sensors, to the empirical performance, assessed via simulations, of the RndEx-PF tracker, and is also compared to the PCRLB for the mean-square state estimation error associated with the optimal centralized filter that assimilates all network measurements at each instant. Finally, we also compare the RndEx diffusion bound to the simulation performance of a standard iterative consensus KL fusion tracker which follows the approach in [2] and of a modified diffusion KL fusion tracker running respectively in non-iterative mode as in [5] and in consensus mode as in [2].

The paper is divided into 7 sections. Section I is this Introduction. In Sec. II, we review briefly the RndEx-PF algorithm and the underlying state and sensor models assumed in the paper. In Sec. III, we introduce the methodology for computation of the PCRLB assuming that the network nodes cooperate using the proposed random exchange protocol. Sec. IV then briefly describes the alternative consensus KL tracker based on [2] and the proposed variation inspired by [5]. Simulation results, are presented in Sec. V. Finally, we offer some conclusions in Sec. VI.

II. RANDOM EXCHANGE DIFFUSION FILTER

In this Section, we review the state and sensor models and the RndEx-PF tracking algorithm from references [6] and [7]. We use lowercase letters to denote both random

ISBN 978-0-9928626-7-1

variables/vectors and realizations of random variables/vectors with the proper interpretation implied in context.

II-A. State and Sensor Model

We track the sequence of hidden state vectors $\{\mathbf{x}_n \triangleq \begin{bmatrix} x_n & \dot{x}_n & y_n & \dot{y}_n \end{bmatrix}^T\}$ that collect the positions and velocities of a moving emitter's centroid respectively in dimensions x and y at each time instant $n \geq 0$. The sequence $\{\mathbf{x}_n\}$ evolves in time according to the linear, white-noise acceleration model $\mathbf{x}_{n+1} = \mathbf{F}\mathbf{x}_n + \mathbf{u}_n$, described in [10], with $\{\mathbf{u}_n\}$ a sequence of independent, identically distributed (i.i.d) Gaussian vectors with zero mean and covariance matrix $\mathbf{Q}$. Moreover, let T and σ_{accel} denote respectivelly the sampling period and the acceleration standard deviation, matrices $\mathbf{F}$ and $\mathbf{Q}$ are given by $\mathbf{F} = diag(\tilde{\mathbf{F}}, \tilde{\mathbf{F}})$ and $\mathbf{Q} = diag(\tilde{\mathbf{Q}}, \tilde{\mathbf{Q}})$ with $\tilde{\mathbf{F}} = \begin{bmatrix} 1 & T \\ 0 & 1 \end{bmatrix}$ and $\tilde{\mathbf{Q}} = \sigma^2_{accel} \begin{bmatrix} T^3/3 & T^2/2 \\ T^2/2 & T \end{bmatrix}$.

A network of R RSS sensors records at each instant n the measurements $z_{n,r}$ in dBm at each network location $r \in \mathcal{V} \triangleq \{1, 2, \ldots, R\}$ such that [11]

$$z_{n,r} = \underbrace{P_0 - 10\zeta_r \log\left(\frac{||\mathbf{H}\mathbf{x}_n - \mathbf{x}_r||}{d_0}\right)}_{g_r(\mathbf{x}_n)} + \nu_{n,r} \qquad (1)$$

where $\nu_{n,r}$ is a zero-mean i.i.d. Gaussian noise process with known variance σ^2_r, $\mathbf{x}_r$ is the r-th sensor position, $||.||$ is the Euclidean norm, and the parameters (P_0, d_0, ζ_r) are known model parameters (see [11] for details) and $\mathbf{H}$ is a 2×4 projection matrix such that $H(1,1) = H(2,3) = 1$ and $H(i,j) = 0$ otherwise. In the remainder of the paper, the *closed* neighborhood of node r, denoted $\mathbf{N}(r)$, is defined as the union of $\{r\}$ and the set of all indices $\{\ell\}$ such that node ℓ is a neighbor of node r according to the topology of the network graph. The measurement noise $\nu_{n,r}$ is also assumed independent from node to node.

II-B. Random Exchange Diffusion Particle Filter

Assume first that a given node $s \in \mathcal{V}$ has at instant $n-1$ a parametric approximation $\tilde{p}_s(\mathbf{x}_{n-1})$ of its local posterior state p.d.f. built from a weighted set of samples $\{w^{(j)}_{n-1,s}, \mathbf{x}^{(j)}_{n-1,s}\}$, $j = 1, \ldots, N_p$, that represents the true posterior p.d.f. $p(\mathbf{x}_{n-1}|\mathcal{Z}_{0:n-1,s})$ where $\mathcal{Z}_{0:n-1,s}$ is the set of network measurements assimilated by s up to instant $n-1$. At instant n, after all network nodes have executed the random exchange protocol originally introduced in [6] and [7] and summarized in Sec. III-A, node s and another random network node r exchange their parametric representations of the state posterior such that $\tilde{p}_s(.)$ is now available at node r. Upon receiving $\tilde{p}_s(.)$, node r at instant n, for $j = 1, \ldots, N_p$,

1) Draws new particles $\tilde{\mathbf{x}}^{(j)}_{n-1,s} \sim \tilde{p}_s(\mathbf{x}_{n-1})$,
2) Samples $\mathbf{x}^{(j)}_{n,r} \sim p(\mathbf{x}_n|\tilde{\mathbf{x}}^{(j)}_{n-1,s})$,
3) Computes the updated importance weights $w^{(j)}_{n,r} \propto \prod_{\ell \in \mathbf{N}(r)} p(z_{n,\ell}|\mathbf{x}^{(j)}_{n,r})$,

where, in Line 3, the proportionality constant is such that $\sum_j w^{(j)}_{n,r} = 1$. Barring the parametric approximation step prior to the random exchange protocol, it can be shown, see [7], that $\{w^{(j)}_{n,r}, \mathbf{x}^{(j)}_{n,r}\}$ is now a properly weighted set to represent the posterior $p(\mathbf{x}_n|\mathcal{Z}_{0:n,r})$ at node r at instant n, where $\mathcal{Z}_{0:n,r} \triangleq \mathcal{Z}_{0:n-1,s} \cup \mathcal{Z}_{n,r}$ and $\mathcal{Z}_{n,r} \triangleq \{z_{n,\ell}, \ell \in \mathbf{N}(r)\}$. Finally, we approximate the integral in $E\{\mathbf{x}_n|\mathcal{Z}_{0:n,r}\}$ by the Monte Carlo approximation

$$\hat{\mathbf{x}}_{n,r} \triangleq \sum_j w^{(j)}_{n,r}\ \mathbf{x}^{(j)}_{n,r}.$$

III. PCRLB FOR THE RNDEX DIFFUSION FILTER

We introduce in this section a methodology to compute the posterior Cramér-Rao lower bound (PCRLB) for the distributed emitter tracking error considering that network nodes diffuse information using the random exchange protocol described in the sequel.

III-A. Random Exchange Protocol

More specifically, at instant $n-1$, each network node s randomly chooses an available neighboring node ℓ and sends then a single request to exchange the parametric representation of its local posterior with node ℓ. Upon receiving an acknowledgement from node ℓ, node s thus sends the set of parameters that represent $\tilde{p}_s(.)$ to node ℓ and, likewise, receives from node ℓ the corresponding set of parameters that represent $\tilde{p}_\ell(.)$. The random exchange procedure terminates when all network nodes have their requests processed by an available node in their vicinity. Finally, after performing the random exchange step, each node r broadcasts its own measurement at instant n to its neighbors and then assimilates the set of measurements $\mathcal{Z}_{n,r}$ using the procedure in Line 3 of Section II-B.

As the initial posterior p.d.f. $p(\mathbf{x}_0|\mathcal{Z}_{0,r_0})$ on a node $r_0 \in \mathcal{V}$ at time 0 follows a path $\boldsymbol{\mathcal{P}}_{n,r_n} \triangleq \{r_0, \ldots, r_k, \ldots, r_n\}$ along the network according to the random exchange protocol, it assimilates, at each time instant $k \in \{0, \ldots, n\}$, the available measurements $\mathcal{Z}_{k,r_k}$ at each visited node $r_k \in \boldsymbol{\mathcal{P}}_{n,r_n}$. Mathematically, at a given time n, the posterior $p(\mathbf{x}_n|\mathcal{Z}_{n,r_n}, \mathcal{Z}_{0:n-1,r_{n-1}})$ at a node r_n is equivalent then (again barring parametric approximations) to the posterior provided by a fusion center that, at each instant $k \in \{0, \ldots, n\}$, randomly chooses a closed neighborhood $\mathbf{N}(r_k)$ and assimilates all observations contained in $\mathcal{Z}_{k,r_k}$. That interpretation plays a crucial role in the derivation of the PCRLB for the state estimation error as discussed in the sequel.

III-B. Computation of the PCRLB

Let $\mathbf{J}_{n,r_n}$ denote the Fisher information matrix at instant n for node r_n conditioned on a particular path realization $\boldsymbol{\mathcal{P}}_{n,r_n}$ along the network. In precise mathematical terms, we write

$$\mathbf{J}_{n,r_n} \triangleq E\left\{-\Delta^{\mathbf{x}_n}_{\mathbf{x}_n} \log p(\mathbf{x}_{0:n}, \mathcal{Z}_{0:n,r_n})|\boldsymbol{\mathcal{P}}_{n,r_n}\right\}, \qquad (2)$$

ISBN 978-0-9928626-7-1 © EURASIP 2017

where $\Delta_{\mathbf{x}}^{\mathbf{x}'} \triangleq \nabla_{\mathbf{x}}\nabla_{\mathbf{x}'}^T$ and $\nabla_{\mathbf{x}} \triangleq \left[\frac{\partial}{\partial x} \quad \frac{\partial}{\partial \dot{x}} \quad \frac{\partial}{\partial y} \quad \frac{\partial}{\partial \dot{y}}\right]^T$ denote respectively the Laplacian and the Jacobian operators. Thus, conditioned on $\boldsymbol{\mathcal{P}}_{n,r_n}$, the posterior Cramér-Rao lower bounds (PCRLB) $\mathbf{P}_{n,r_n} \triangleq (\mathbf{J}_{n,r_n})^{-1}$ for the estimate $\hat{\mathbf{x}}_{n,r_n}$ computed by node r_n satisfies the inequality

$$E\left\{||\hat{\mathbf{x}}_{n,r_n} - \mathbf{x}_n||^2 \mid \boldsymbol{\mathcal{P}}_{n,r_n}\right\} \geq \text{tr}[\mathbf{P}_{n,r_n}], \tag{3}$$

where tr[.] denotes the trace of a matrix. Additionally, provided the usual independence assumptions

$$\begin{aligned} p(\mathcal{Z}_{k,r_k}|\mathbf{x}_{0:k}, \mathcal{Z}_{0:k-1,r_{k-1}}) &= p(\mathcal{Z}_{k,r_k}|\mathbf{x}_k) \\ p(\mathbf{x}_k|\mathbf{x}_{0:k-1}, \mathcal{Z}_{0:k-1,r_{k-1}}) &= p(\mathbf{x}_k|\mathbf{x}_{k-1}) \end{aligned}$$

for $0 \leq k \leq n$, the joint probability of $\mathbf{x}_{0:n} \triangleq (\mathbf{x}_0, \ldots, \mathbf{x}_n)$ and $\mathcal{Z}_{0:n,r_n} \triangleq \mathcal{Z}_{0,r_0} \cup \ldots \cup \mathcal{Z}_{n,r_n}$ can be factorized as

$$p(\mathbf{x}_{0:n}, \mathcal{Z}_{0:n,r_n}) = p(\mathbf{x}_0) \prod_{k=0}^{n} p(\mathcal{Z}_{k,r_k}|\mathbf{x}_k) \prod_{k=1}^{n} p(\mathbf{x}_k|\mathbf{x}_{k-1}).$$

We can apply therefore the method introduced in [9] to recursively compute the Fisher matrix $\mathbf{J}_{n+1,r_{n+1}}$ at instant $n+1$ given the Fisher matrix $\mathbf{J}_{n,r_n}$ originated from a node r_n and the set of measurements $\mathcal{Z}_{n+1,r_{n+1}}$ available at node r_{n+1}.

We extend first the recursive equations derived in [9] to consider multiple observers as in (1) and write

$$\mathbf{J}_{n+1,r_{n+1}} = \mathbf{D}_n^{22} - \mathbf{D}_n^{21}(\mathbf{J}_{n,r_n} + \mathbf{D}_n^{11})^{-1}\mathbf{D}_n^{12} \tag{4}$$

where

$$\begin{aligned} \mathbf{D}_n^{11} &= E\{-\Delta_{\mathbf{x}_n}^{\mathbf{x}_n} \log p(\mathbf{x}_{n+1}|\mathbf{x}_n)\} & (5) \\ \mathbf{D}_n^{12} &= E\{-\Delta_{\mathbf{x}_n}^{\mathbf{x}_{n+1}} \log p(\mathbf{x}_{n+1}|\mathbf{x}_n)\} = \left[\mathbf{D}_n^{21}\right]^T & (6) \\ \mathbf{D}_n^{22} &= E\{-\Delta_{\mathbf{x}_{n+1}}^{\mathbf{x}_{n+1}} \log p(\mathbf{x}_{n+1}|\mathbf{x}_n)\} \\ &+ E\{-\Delta_{\mathbf{x}_{n+1}}^{\mathbf{x}_{n+1}} \log p(\mathcal{Z}_{n+1,r_{n+1}}|\mathbf{x}_{n+1})\}. & (7) \end{aligned}$$

Furthermore, since the measurements in $\mathcal{Z}_{n+1,r_{n+1}}$ are independent, we can further write

$$\log p(\mathcal{Z}_{n+1,r_{n+1}}|\mathbf{x}_{n+1}) = \sum_{\ell \in \mathbf{N}(r_{n+1})} \log p(z_{n+1,\ell}|\mathbf{x}_{n+1}). \tag{8}$$

Next, we rewrite (5), (6) and (7) for the particular filtering problem introduced in Sec. II-A with linear dynamics and log-normal observation model (1)

$$\begin{aligned} \mathbf{D}_n^{11} &= \mathbf{F}^T\mathbf{Q}^{-1}\mathbf{F} & (9) \\ \mathbf{D}_n^{12} &= -\mathbf{F}^T\mathbf{Q}^{-1} = \left[\mathbf{D}_n^{21}\right]^T & (10) \\ \mathbf{D}_n^{22} &= \mathbf{Q}^{-1} + \sum_{\ell \in \mathbf{N}(r_{n+1})} \sigma_\ell^{-2} E\{\left[\nabla_{\mathbf{x}_{n+1}} g_\ell^T(\mathbf{x}_{n+1})\right] \\ &\times \left[\nabla_{\mathbf{x}_{n+1}} g_\ell^T(\mathbf{x}_{n+1})\right]^T\} & (11) \end{aligned}$$

where

$$\left[\nabla_{\mathbf{x}} g_\ell^T(\mathbf{x})\right]\left[\nabla_{\mathbf{x}} g_\ell^T(\mathbf{x})\right]^T = \left(\frac{10\zeta_\ell}{\ln 10}\right)^2 \frac{\mathbf{D}_{\mathbf{x},\ell}}{\|\mathbf{H}\mathbf{x} - \mathbf{x}_\ell\|^4} \tag{12}$$

with $\mathbf{D}_{\mathbf{x},\ell}(1,1) = (x - x_\ell)^2$, $\mathbf{D}_{\mathbf{x},\ell}(3,3) = (y - y_\ell)^2$, $\mathbf{D}_{\mathbf{x},\ell}(1,3) = \mathbf{D}_{\mathbf{x},\ell}(3,1) = (x - x_\ell)(y - y_\ell)$ and $\mathbf{D}_{\mathbf{x},\ell}(i,j) = 0$ otherwise.

Note that, as opposed to (9) and (10), Eq. (11) does not have an exact closed form solution. Thus, we simulate several emitter trajectories $\mathbf{x}_{0:n+1}^{(i)}$, $i \in \{1, \ldots, N_T\}$, according to the emitter dynamic model and use the following Monte Carlo approximation to compute the expectation in the right-hand side of (11)

$$\mathbf{D}_n^{22} \approx \mathbf{Q}^{-1} + \sum_{\ell \in \mathbf{N}(r_{n+1})} \left(\frac{10\zeta_\ell}{\ln 10\, \sigma_\ell}\right)^2 \frac{1}{N_T} \sum_{i=1}^{N_T} \frac{\mathbf{D}_{\mathbf{x}_{n+1}^{(i)},\ell}}{\left\|\mathbf{H}\mathbf{x}_{n+1}^{(i)} - \mathbf{x}_\ell\right\|^4}. \tag{13}$$

Now, let $\mathbf{P}_{n,r_n}^\star$ denote the unconditioned PCRLB for each node r_n at instant n such that

$$E\left\{||\hat{\mathbf{x}}_{n,r_n} - \mathbf{x}_n||^2\right\} \geq \text{tr}[\mathbf{P}_{n,r_n}^\star] \triangleq \text{tr}[(\mathbf{J}_{n,r_n}^\star)^{-1}], \tag{14}$$

where $\mathbf{J}_{n,r_n}^\star$ is the unconditioned Fisher information matrix at instant n. From the law of total expectation and Eq. (2), we can write

$$\begin{aligned} \mathbf{J}_{n,r_n}^\star &\triangleq E\left\{-\Delta_{\mathbf{x}_n}^{\mathbf{x}_n} \log p(\mathbf{x}_{0:n}, \mathcal{Z}_{0:n,r_n})\right\} \\ &= E\left\{E\left\{-\Delta_{\mathbf{x}_n}^{\mathbf{x}_n} \log p(\mathbf{x}_{0:n}, \mathcal{Z}_{0:n,r_n})|\boldsymbol{\mathcal{P}}_{n,r_n}\right\}\right\} \\ &= E\left\{\mathbf{J}_{n,r_n}\right\} \end{aligned} \tag{15}$$

with the expectation in (15) taken over all possible paths $\boldsymbol{\mathcal{P}}_{n,r_n}$ along the network that end at node r_n at instant n.

Finally, we compute a *Monte Carlo approximation* of $\mathbf{J}_{n,r_n}^\star$ in (15) by averaging out a large number N_f of Fisher matrices $\mathbf{J}_{n,r_n}^{(m)}$ conditioned on distinct path realizations $\boldsymbol{\mathcal{P}}_{n,r_n}^{(m)}$ induced by the random exchange protocol, i.e.

$$\mathbf{J}_{n,r_n}^\star \approx \frac{1}{N_f} \sum_{m=1}^{N_f} \mathbf{J}_{n,r_n}^{(m)}.$$

IV. KULLBACK-LEIBLER FUSION

Assume, as before, that a given node r has at instant $n-1$ a weighted set of particles $\{w_{n-1,r}^{(j)}, \mathbf{x}_{n-1,r}^{(j)}\}$, $j = 1, \ldots, N_p$, that represents its current posterior belief about the unknown target state. The application of the consensus KL fusion procedure detailed in [2] and briefly described in Sec. I would entail the following steps at instant n at each node $r \in \mathcal{V}$:

1) For $j = 1, \ldots, N_p$ sample $\tilde{\mathbf{x}}_{n,r}^{(j)} \sim p(\mathbf{x}_n|\mathbf{x}_{n-1,r}^{(j)})$ and update the weights as $\tilde{w}_{n,r}^{(j)} \propto w_{n-1,r}^{(j)} p(z_{n,r}|\tilde{\mathbf{x}}_{n,r}^{(j)})$ with $\sum_j \tilde{w}_{n,r}^{(j)} = 1$.
2) Build a parametric approximation $\tilde{p}_r(\mathbf{x}_n)$ using the sample set $\{\tilde{w}_{n,r}^{(j)}, \tilde{\mathbf{x}}_{n,r}^{(j)}\}$ and make $\beta_r^{(0)}(\mathbf{x}_n) = \tilde{p}_r(\mathbf{x}_n)$.
3) For $k = 1, \ldots, K_{\max}$, make

$$\beta_r^{(k+1)}(\mathbf{x}_n) \propto \prod_{\ell \in \mathbf{N}(r)} [\beta_\ell^{(k)}(\mathbf{x}_n)]^{a_{r,\ell}}, \quad a_{r,\ell} \geq 0$$

with $\sum_{\ell \in \mathbf{N}(r)} a_{r,\ell} = 1$, $a_{r,\ell} = a_{\ell,r}$, and $\int \beta_r^{(k+1)}(\mathbf{x}) d\mathbf{x} = 1$.

ISBN 978-0-9928626-7-1 © EURASIP 2017

4) For $j = 1, \ldots, N_p$, resample $\mathbf{x}_{n,r}^{(j)} \sim \beta_r^{(K\text{max})}(\mathbf{x}_n)$ and reset $w_{n,r}^{(j)} = 1/N_p$.

It is relatively straightforward to show that $\lim_{k\to\infty} \beta_r^{(k)}(\mathbf{x}_n) \propto [\prod_{\ell\in\mathcal{V}} \tilde{p}_\ell(\mathbf{x}_n)]^{1/R}$, $\forall r$, which, as argued in [2], is, after normalization, the p.d.f. p^* that minimizes $(1/R)\sum_{\ell\in\mathcal{V}} \mathcal{D}(p^*||\tilde{p}_\ell)$, where $\mathcal{D}(.||.)$ denotes the Kullback-Leibler divergence.

Modified Version We modify the KL fusion algorithm replacing the weight update rule in Line 1 with $\tilde{w}_{n,r}^{(j)} \propto w_{n-1,r}^{(j)} \prod_{\ell\in\mathbf{N}(r)} p(z_{n,\ell}|\tilde{\mathbf{x}}_{n,r}^{(j)})$ to allow network nodes to assimilate the available measurements in their vicinity before the K_{max} consensus iterations. In addition, following the lead in [5], we can optionally make the algorithm non-iterative by setting $K_{\text{max}} = 1$ in Line 3. As shown in [5], the choice of $K_{\text{max}} = 1$ leads to $\beta_r^{(1)}(\mathbf{x}_n)$ on the left-hand side of the recursion in Line 3 to be the p.d.f. p that minimizes instead $\sum_{\ell\in\mathbf{N}(r)} a_{r,\ell}\, \mathcal{D}(p||\tilde{p}_\ell)$.

If $\beta_r^{(k)}(.)$ is represented at the iteration k and at node r by a Gaussian function with mean vector $\mathbf{m}_r^{(k)}$ and covariance matrix $\mathbf{P}_r^{(k)}$, the fusion rule in Line 3 reduces [5] to making $[\mathbf{P}_r^{(k+1)}]^{-1} = \sum_{\ell\in\mathbf{N}(r)} a_{r,\ell} (\mathbf{P}_\ell^{(k)})^{-1}$ and

$$(\mathbf{P}_r^{(k+1)})^{-1}\mathbf{m}_r^{(k+1)} = \sum_{\ell\in\mathbf{N}(r)} a_{r,\ell}\, (\mathbf{P}_\ell^{(k)})^{-1}\mathbf{m}_\ell^{(k)}.$$

V. SIMULATION RESULTS

We assessed the performance of the RndEx-PF tracker using 100 independent Monte Carlo runs in a simulated scenario consisting of $R = 25$ RSS sensors over a simulation period of 100 s. We used the same simulation parameters described in [6] to simulate the emitter dynamics and generate sensor measurements. We assumed a Gaussian initial state distribution $p(\mathbf{x}_0)$ with mean $\bar{\mathbf{x}}_0 = \begin{bmatrix}50\,\text{m} & 0\,\text{m/s} & 50\,\text{m} & 0\,\text{m/s}\end{bmatrix}^T$ and covariance matrix $\mathbf{P}_0 = diag(\begin{bmatrix}(5\,\text{m})^2 & (0.05\,\text{m/s})^2 & (5\,\text{m})^2 & (0.05\,\text{m/s})^2\end{bmatrix})$. At any given node r_0, we initialized the conditioned Fisher matrix as $\mathbf{J}_{0,r_0} = \mathbf{P}_0^{-1}$.

All filters employed $N_p = 1000$ particles. The particles at each node were initialized at instant 0 according to the distribution $p(\mathbf{x}_0)$. At instant $n+1$, we used a distinct set of $N_T = 10000$ trajectories in (13) to recursively compute the conditioned Fisher matrix $\mathbf{J}_{n+1,r_{n+1}}$ at node r_{n+1} given the Fisher matrix $\mathbf{J}_{n,r_n}$ at node r_n. Finally, at any instant n, we employed $N_f = 1000$ different Fisher matrices $\{\mathbf{J}_{n,r_n}^{(m)}, 1 \leq m \leq N_f\}$ conditioned on distinct network paths $\boldsymbol{\mathcal{P}}_{n,r_n}^{(m)}$ to compute the unconditioned Fisher matrix $\mathbf{J}_{n,r_n}^\star = (\mathbf{P}_{n,r_n}^\star)^{-1}$ at node r_n.

Note that, in the RndEx filter, each node has a different position estimate and a different associated mean-square estimation error (MSEE). Fig. 1 shows the RndEx-PF empirical root-mean-square (RMS) position estimate error averaged over all network nodes from instant zero up to instant 100 s and compares it to the average PCRLB for the square-root of the RndEx filter position MSEE obtained by averaging $\sqrt{\mathbf{P}_{n,r_n}^\star(1,1) + \mathbf{P}_{n,r_n}^\star(3,3)}$ over all possible 25 node indices r_n at each instant n. For comparison, we also show in Fig. 1 the PCRLB for the square-root of the centralized filter position MSEE, and the average RMS position estimate error curves for the Consensus KL Fusion filter [2] using $K_{\text{max}} = 10$ consensus iterations and for the modified KL fusion algorithm proposed in Sec. IV using either $K_{\text{max}} = 1$ and $K_{\text{max}} = 10$ consensus iterations. We refer to the modified trackers with $K_{\text{max}} = 1$ and $K_{\text{max}} = 10$ as the Non-iterative and the Iterative KL Fusion filters, respectively. The KL fusion trackers used Metropolis weights $a_{r,\ell}$ [12], [13] and the bars shown in Fig. 1 along the curves represent the standard deviation of the error norm across all nodes. An alternative algorithm for distributed computation of the optimal centralized PCRLB is discussed in [14].

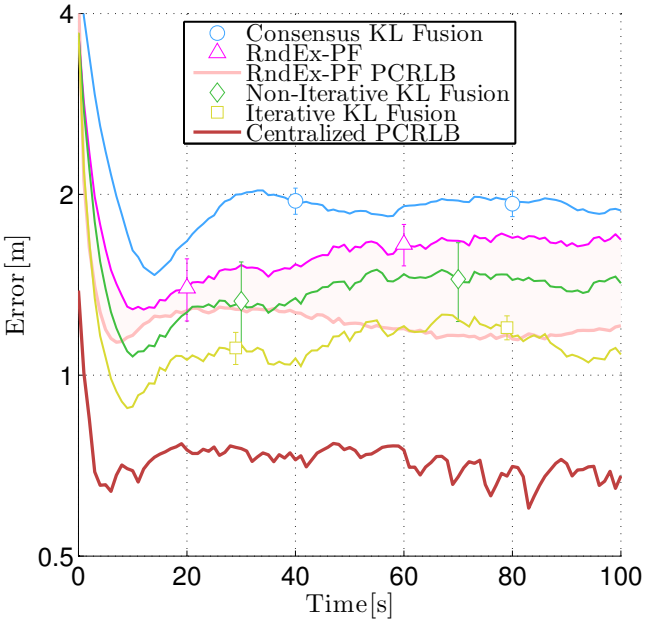

Fig. 1. Evolution of the estimated position RMS error norm.

As expected, the RndEx-PF RMS error is above its corresponding PCRLB. The region between the empirical RndEx-PF RMS error curve and its PCRLB in Fig. 1 is filled in light red to highlight the gap between the two curves. Furthermore, despite being non-iterative, the RndEx-PF tracker actually showed better error performance in our simulations than the standard Consensus KL Fusion algorithm, probably because the latter does not include local cooperation before fusion. However, RndEx-PF had a higher RMS error than the Non-iterative KL Fusion algorithm with $K_{\text{max}} = 1$, which suggests that local cooperation plus KL fusion allows nodes to incorporate more information at each time than the random exchange protocol. The performance of the modified

ISBN 978-0-9928626-7-1 © EURASIP 2017

KL fusion scheme was further improved by increasing $K_{\max}$ from 1 to 10, in which case the corresponding RMS error curve further approaches the PCRLB for the centralized filter error. Note also that the performance of the modified KL fusion tracker is *not* limited by the theoretical RndEx-PF PCRLB as KL fusion is a different algorithm.

Table I summarizes the performance metrics for each evaluated algorithm. They were computed according to the methodology previously introduced in [6]. The RndEx-PF tracker has half of the average reception (RX) communication cost per node of the modified Non-Iterative KL Fusion algorithm with a similar processing cost and at the expense of a slight degradation in error performance. In turn, in addition to having a worse error performance, the Consensus KL Fusion tracker has an average RX communication cost one order of magnitude higher than that of RndEx-PF employing however roughly one-third of the processing cost. Finally, the Iterative KL Fusion tracker has better error performance than the Consensus KL Fusion algorithm at the expense of a slight increase in the average transmission (TX) communication cost and a huge increase of 170 % in processing cost since the nodes assimilate all measurements in their vicinity.

Table I. Communication and processing performances.

Evaluated Algorithm	RX Rate	TX Rate	Duty Cycle
RndEx-PF	148 B/s	132 B/s	2.9 %
Non-Iterative KL Fusion	317 B/s	64 B/s	2.6 %
Iterative KL Fusion	2.9 KB/s	604 B/s	2.7 %
Consensus KL Fusion	2.9 KB/s	600 B/s	1.0 %

VI. CONCLUSIONS

We computed the PCRLB for the MSEE of a distributed, random exchange (RndEx) diffusion filter. The RndEx PCRLB was compared to the centralized filter PCRLB and to the empirical error of a Gaussian PF implementation of the RndEx filter, denoted RndEx-PF. In addition, we also compared the RndEx empirical error and the centralized PCRLB's to the empirical error of three KL fusion filters. The error curve of the RndEx-PF tracker, as expected, was above its corresponding PCRLB. On the other hand, the Consensus KL Filter without local cooperation before fusion performed worse than RndEx-PF with a communication cost one order of magnitude higher than that of RndEx-PF, which suggests that, in the evaluated scenario, local cooperation is preferable to standard consensus cooperation. However, the Non-iterative KL Filter with local cooperation before fusion was close to the RndEx PCRLB with a communication cost only twice as high as that of RndEx-PF. Finally, by enabling local cooperation before consensus KL fusion, the Iterative KL Filter, although still worse than the centralized PCRLB, outperformed the RndEx PCRLB.

VII. REFERENCES

[1] O. Hlinka, F. Hlawatsch, and P. M. Djuric, "Distributed Particle Filtering in Agent Networks: A Survey, Classification, and Comparison," *IEEE Signal Processing Magazine*, vol. 30, no. 1, pp. 61–81, January 2013.

[2] L. Chisci, G. Battistelli, C. Fantacci, A. Farina, and B.-N. Vo, "Average Kullback-Leibler divergence for random finite sets," *Proc. 18th Int'l Conf. on Information Fusion*, Washington, D.C., July 6-9, 2015.

[3] M. B. Guldogan, "Consensus Bernoulli filter for distributed detection and tracking using multi-static Doppler shifts," *IEEE Signal Processing Letters*, vol. 6, no. 21, pp. 672–676, 2014.

[4] L. Xiao and S. Boyd, "Fast linear iterations for distributed averaging," *Syst. Control Letters*, vol. 53, no. 1, pp. 65–78, September 2004.

[5] K. Dedecius and P. M. Djuric, "Diffusion filtration with approximate Bayesian computation," *Proc. 2015 IEEE Int. Conf. on Acoustics, Speechm and Signal Processing*, pp. 3207-3211, Brisbane QLD, Australia, April 2015.

[6] S. S. Dias, and M. G. S. Bruno, "Distributed Emitter Tracking using Random Exchange Diffusion Particle Filters," *16th International Conference on Information Fusion*, Istanbul, Turkey, July 2013.

[7] M. G. S. Bruno and S. S. Dias, "Cooperative emitter tracking using Rao-Blackwellized random exchange diffusion particle filters," *Eurasip Journal on Advances in Signal Processing*, 2014:19, pp. 1–18, February 2014, doi: 10.1186/1687-6180-2014-19.

[8] S. Kar and J. M. F. Moura, "Gossip and distributed Kalman filtering: weak consensus under weak detectability," *IEEE Transactions on Signal Processing*, vol. 59, no. 4, pp. 1766–1784, April 2011.

[9] P. Tichavský, C. H. Muravchik, and A. Nehorai, "Posterior Cramér-Rao Bounds for Nonlinear Discrete-Time Filtering," *IEEE Transactions on Signal Processing*, vol. 46. no. 5, pp. 1386-1396, May 1998.

[10] Y. Bar-Shalom and X. Li, "Multitarget-Multisensor Tracking: Principles and Techniques," YBS, Storrs, CT, 1995.

[11] N. Patwari, A. O. Hero III, M. Perkins, N. S. Correal, and R. J. O'Dea, "Relative location estimation in wireless sensor networks," *IEEE Transactions on Signal Processing*, vol. 51, n. 3, pp. 2137-2148, March 2003.

[12] L. Xiao, S. Boyd, and S. Lall, A scheme for robust distributed sensor fusion based on average consensus, in IEEE Int. Conf. Info. Processing in Sensor Networks (ISPN), 2005.

[13] F. Cativelli and A. Sayed, "Diffusion LMS Strategies for Distributed Computation," *IEEE Transactions on Signal Processing*, vol. 58. no.3, pp.1035-1048, March 2010.

[14] A. Mohammadi and A. Asif, "Distributed Posterior Cramér-Rao Lower Bound for Nonlinear Sequential Bayesian Estimation, " *2012 IEEE 7th Sensor Array and Multichannel Signal Processing Workshop (SAM)*, pp. 509-512, Hoboken NJ, U.S.A., June 2012.

ISBN 978-0-9928626-7-1 © EURASIP 2017